Proceedings of the 21st ICSMGE, Vienna, Austria, 14 – 19 June 2026. Pistrol, Adam & Schweiger (eds.)
Published by: ÖGG, Austrian Society for Geomechanics, Salzburg, Austria, ISBN 978-3-9503898-4-5
https://doi.org/10.53243/ICSMGE2026-786

Measurement and modeling of the temperature-dependent thermal conductivity of freezing to thawing sands

Aashish Pokhrel, **Xinbao Yu,** Laureano R. Hoyos
Department of Civil Engineering, University of Texas at Arlington, TX, USA, xinbao@uta.edu

ABSTRACT: While modeling geothermal structures, such as energy piles, and the coupled heat and moisture movements, accurate estimates of thermal conductivity and its temperature dependence is required. However, the thermal conductivity of the soil samples is typically measured at room temperature, and its temperature dependence, especially at freezing conditions, is estimated using the pre-established empirical formulations. Thus, this research aimed to study the combined effect of moisture content and temperature on the sandy soils in a temperature-controlled environment using two soil types: Benbrook sand (SM) with non-plastic fines and a fine-grained Ottawa sand (ASTM C778). The thermal conductivity of the soil samples at varying moisture content was measured from freezing (-10°C) to the thawed stage at elevated temperatures (60°C). The tests were performed in a heat cell with cylindrical soil specimens measuring 8.89 cm in diameter and 10.16 cm in height. The thermal conductivity was measured independently using two methods: the transient probe method with the KD-2 probe at room temperature, and the steady-state method at varying temperatures in the heating cell, with one-dimensional heat flux maintained. The results from the laboratory tests allowed evaluation of soil freezing models for predicting unfrozen water content and thermal conductivity functions in freezing and thawed soils.

KEYWORDS: Thermal conductivity, freezing soil, thermal conductivity models, SFCC.

1 INTRODUCTION

Accurate prediction of soil thermal conductivity under freezing and thawed conditions has been crucial for modeling geothermal systems, buried infrastructures, artificial ground freezing, and geothermal slope stability in high-temperature and permafrost-affected regions (Farouki, 1981; Alzoubi *et al.*, 2020; Laloui and Di Donna, 2013)**.** With the increasing infrastructure development in cold climates, understanding the soil properties under freezing and thawing conditions has become significantly critical for safe and efficient structural and geothermal designs. (Goering, 2003; Hjort *et al.*, 2022).

The thermal conductivity of freezing soils is affected by the water-ice phase change below the freezing point and the presence of unfrozen water below 0°C (Lunardini, 1988; Orakoglu Firat, 2021). These factors introduce significant complexity when predicting the unfrozen water content and thermal conductivity of the soils below the freezing temperatures (Tarnawski *et al.*, 2011). Furthermore, the ubiquitous use of transient methods for thermal conductivity measurement has led to some unpredictability in the thermal conductivity measurement of the soil, mainly arising due to the melting of ice during the measurement and heat loss in the air voids between the thermal conductivity probes and the surrounding soil (Putkonen, 2003; Alrtimi *et al.*, 2014). Steady–state techniques, although being more labor-intensive and time-consuming, overcome these issues due to the establishment of a steady-state water-ice interface during thermal conductivity measurement. Furthermore, the direct use of Fourier's law of heat transfer for the thermal conductivity measurement leads to minimized errors due to the avoidance of computational assumptions (Farouki, 1981; Sivaprasad and Basu, 2023).

Numerous theoretical, empirical, and machine learning based models have been developed for the prediction of the thermal conductivity of unsaturated soils under freezing conditions. Johansen's (1977) model and its modification by Côté and Konrad (2005) remains one of the most common prediction models with improved accuracy via the inclusion of porosity and minerology. Tarnawski and Wagner (1993) extended the predictive capability across the large temperature range from -30°C to 90°C. Chen et al. (2025) and Zhao et al. (2022) achieved a very high accuracy in thermal conductivity prediction through machine learning algorithms. Recent works by Fu et al. (2023) linked the thermal conductivity model parameters to water retention parameters of the soil, further aiding in geothermal analysis.

Parallelly, Soil Freezing Characteristics Curve (SFCC) models have been developed for the prediction of the unfrozen water content in freezing soils. Anderson and Tice (1972) and Kozlowski (2007) developed an exponential-based function for the unfrozen water content prediction. Later, Spaans and Baker (1996) furthered the model by introducing thermodynamics and capillarity, which further related SFCC to soil texture and suction pressure. Van Genuchten's (1980) water retention framework was modified by Liu and Yu (2013) to introduce a sigmoidal framework for more accurate SFCC model development. The recent model by Jin et al. (2020) employs the specific surface area of the solids and temperature to predict the unfrozen water content of the soil. Most of the developed SFCC models work under saturated conditions, which is a rare case in everyday life, making Liu and Yu (2013) model a more practical SFCC model for unsaturated soils.

Despite significant advances in thermal-conductivity functions and SFCC models, most models are validated on limited datasets. Furthermore, the use of thermal conductivity data from the transient probe method makes the models less reliable, especially under freezing temperatures, due to the shortcomings of the transient probe method. Thus, this paper aims to: (1) measure the thermal conductivity and unfrozen water content of sandy soils from freezing to elevated temperatures, (2) evaluate common SFCC models, and (3) evaluate the previously developed thermal conductivity models.

2 METHODOLOGY

2.1 *Fully Instrumented Heating Cell*

The heating cell consists of two concentric acrylic cylinders with an inside diameter of 8.89 cm (3.5 in) and 20.96 cm (8.25 in), and wall thicknesses of 0.635 cm (0.25 in). The apparatus has a height of 10.16 cm (4 in) with custom-sized holes on the walls for sensor installation. The soil samples in the inner cylinder are used for the thermal properties' measurement, while the outer cylindrical sample acts as a buffer zone between the inner soil sample and the outer fiberglass insulation to

prevent radial heat transfer from the measuring soil sample. Furthermore, the heat cell is equipped with independent heat exchangers at the top and bottom of the heat cell, parallel to induce one-dimensional heat movement in the soil sample. The heat exchanger systems consist of a copper plate for efficient heat transfer to the soil and consist of spiral square channels (0.65 cm x 0.65 cm cross section) with inlet and outlet valves, as shown in the schematic in Figure 1 and picture in Figure 2.

Custom-sized holes are drilled on the side of the heating cell to install the required sensors. The installed sensors comprise thermocouples, custom-calibrated dielectric sensors, and heat flux sensors. The EC-5 sensors (*Meter Group Inc., WA, US*) were custom-calibrated against the known liquids to predict the apparent dielectric permittivity of the soil during the freezing process. Two heat flux sensors, FHF05SC (*HuskefluxUSA Inc., NY, US*), were used to measure the one-dimensional heat flux through the soil column during the steady state to calculate the thermal conductivity of the soil samples. The type-T thermocouples (*Omega Engineering, In, US*) were used to monitor the temperature of the soil and calculate the temperature gradient during the test. The approximate locations of the installed sensors are shown in Figure 2**.**

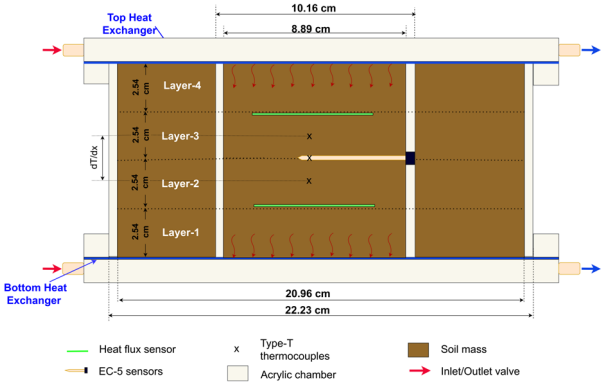

Figure 1. Schematics of a fully instrumented heating cell.

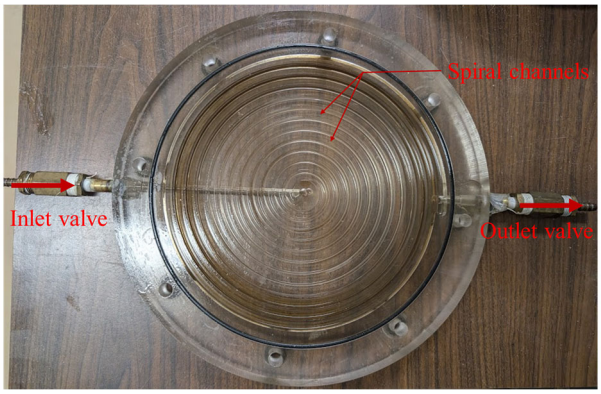

Figure 2. Picture showing the spiral channels of the top heat exchanger.

2.2 *Specimen Preparation*

The apparatus was designed to test the disturbed samples, as it requires compaction and proper sensor installation. Two soil samples, one soil from Benbrook, TX, US, and the second fine-graded Ottawa Sand (ASTM C778), were used. The gradation of the respective soils is shown in Figure 3 below, and the soils were classified as silty sand (SM) with non-plastic fines and poorly graded sand (SP), respectively, based on the USCS soil classification system (ASTM D2487, 2017).

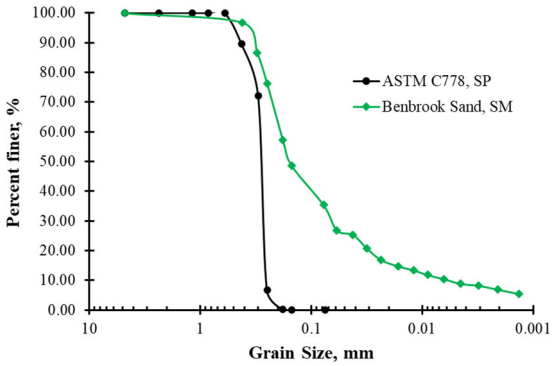

Figure 3. Soil gradation curve for Benbrook and ASTM C778 sands.

The soil samples were prepared to reach the targeted water content and placed in a temperature and humidity-controlled room for 24 hours before sample preparation to facilitate the moisture equilibrium. The soil samples were compacted in four layers with dynamic compaction using gentle tamping to prevent damage to the sensor while establishing good soil–sensor contact. The sensor installation holes were then filled up with silicon–based putty and covered with duct tape to prevent moisture loss to the atmosphere during the test. The soil samples were targeted for a dry density of 1.60 g/cm^3, but some fluctuation in density was present due to dynamic compaction and varying moisture content.

2.3 *Thermal Conductivity Determination*

The fully instrumented heating cell uses a steady-state method to evaluate the thermal conductivity of the soils based on the average heat flux ($q\ W/m^2$) from the two heat flux sensors and temperature gradient (dT/dx) based on thermocouples. Fourier's law of one-dimensional heat transfer was directly applied to calculate the thermal conductivity of the soils. The steady state was attained when the temperature recorded by the thermocouples didn't change by more than $0.05°C$ over an hour. The average of more than an hour of sensor data after attaining the steady state was considered for thermal conductivity calculation by the following equation:

$$q = -k \times \frac{dT}{dx} \quad (1)$$

k: Thermal Conductivity (W/(m.°C), dT/dx: Temperature gradient (°C/m).

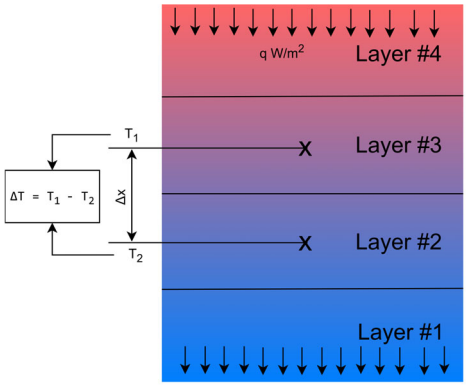

Figure 4. The schematic representation of the temperature gradient and heat flux in the soil column.

The temperature gradient term (dT/dx) in (1) was obtained based on the spacing between top and bottom thermocouples

$(\Delta x, m)$ and their temperature difference $(\Delta T, °C)$ as shown in Figure 4 and given by:

$$\frac{dT}{dx} = \frac{\Delta T}{\Delta x} \quad (2)$$

2.4 *Unfrozen Water Content*

Accurate prediction of unfrozen water content in freezing soil is important for estimating soil properties. In this study, one EC-5 sensor was custom-calibrated against standard liquids (deionized water, Ethanol, Methanol, Acetone, and air) to measure the apparent dielectric constant of the soil during the test. The measured apparent dielectric of the soil was used to calculate the fraction of unfrozen water content in the soil based on the volumetric dielectric mixing formula from Weir (1974), which is given as:

$$\epsilon_{mix} = \sum V_i \epsilon_i^{1/2} \quad (3)$$

ϵ_{mix} = apparent dielectric of the mix; ϵ_i = apparent dielectric of the constituent; V_i = volume fraction of the constituent.

The individual constituents included solids, frozen water, unfrozen water, and air voids for the freezing soil. The custom calibration of EC-5 probes for the apparent dielectric permittivity measurement is provided in Figure 5.

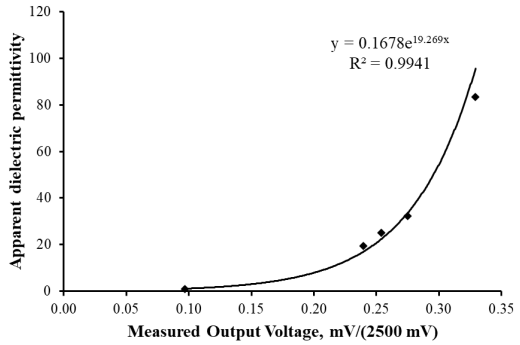

Figure 5. Calibration of EC-5 sensor for apparent dielectric permittivity.

3 THERMAL CONDUCTIVITY AND UNFROZEN WATER CONTENT MODELS

The measured thermal conductivity from the lab test under freezing and elevated temperatures was fit to the geometric mean model from Côté and Konrad (2005), exponential models from Wang et al. (2017), and the Hyperbolic model from Bi et al. (2023). The models were best fit using parameter optimization to assess their ability to predict thermal conductivity in Benbrook sand and fine sand under thawed and freezing conditions.

3.1 *Côté and Konrad Model*

Côté and Konrad's model (2005) uses the geometric mean of solids, frozen water, and unfrozen water with their respective volume fraction in the freezing and thawed soils as given by:

$$\lambda_{sat(f)} = \lambda_s^{1-n_f} \lambda_i^{n_f-\theta_u} \lambda_w^{\theta_u}$$

$\lambda_{sat(f)}$ = thermal conductivity of freezing soil; $\lambda_s, \lambda_i, \lambda_w$ = thermal conductivity of solids, ice, and water; n_f = porosity; θ_u = unfrozen water content.

3.2 *Wang et al. Model*

Wang et al. (2017) developed a model to estimate the thermal conductivity of frozen soils using an exponential equation that takes thermal conductivity of the dry soil, ice, and saturation into consideration, which is given by:

$$\lambda = \lambda_{dry} + (\lambda_{sat} - \lambda_{dry}) \exp\left[0.36\left(1 - \frac{1}{S}\right)\right] + \lambda_i$$
$$\lambda_{sat} = 0.5^n (7.7^q 2.0^{1-q})^{1-n}$$
$$\lambda_{dry} = \frac{0.135\rho_d + 64.7}{2700 - 0.947\rho_d}$$
$$\lambda_i = 2.2\theta_i$$

λ = Thermal conductivity of soil; $\lambda_{dry}, \lambda_{sat}$ = minimum and maximum thermal conductivity of soil; λ_i = thermal conductivity of ice; q = quartz content; n = porosity; S = saturation; θ_i = ice content.

3.3 *Bi et al. Model*

Bi et al. (2023) developed a hyperbolic model for the estimation of thermal conductivity of frozen soils based on temperature and thermal conductivity at 0°C as the input parameters, and two optimization parameters as given by:

$$\lambda = \lambda_{(0°C)}\left[1 + \frac{(-T)}{\alpha + \beta(-T)}\right]$$

λ = Thermal conductivity at T°C; $\lambda_{(0°C)}$ = thermal conductivity of soil at $0°C$; T = temperature ($\leq 0°C$); α, β = optimization parameters.

Furthermore, the unfrozen water content was best fitted in two SFCC models. The first one included the derived version of van Genuchten SWCC by Liu and Yu (2013). The second model includes the exponential model from Kozlowski (2007), which uses three different temperature ranges for unfrozen water content prediction.

3.4 *Liu and Yu Model*

Liu and Yu's model (2013) consists of an updated van Genuchten SWCC model that considers different parameters for the estimation of unfrozen water content at varying temperatures, given by:

$$T(S) = 273.15 \exp\left\{-\frac{1}{3.34 \times 10^8 \alpha}[(S_M S_H - S_M S_L + S_L)\text{^}(-1/m) - 1]^{1/n}\right\}$$

T(S) = Temperature at saturation 'S', K; α, m, n, S_L, S_H = optimization parameters; S_M = effective saturation of unfrozen water in freezing soils.

3.5 *Kozlowski Model*

Kozlowski's (2007) model consists of unfrozen water content in three distinct temperature ranges as given by:

$$w_u = \begin{cases} w \; for \; T > T_f \\ w_{nf} + (w - w_{nf}) \exp\left(-3.35\left(\frac{T_f - T}{T - T_m}\right)^{0.37}\right) \; for \; T_m < T \leq T_f \\ w_{nf} \; for \; T \leq T_m \end{cases}$$

w_u = Unfrozen water content; w_{nf} = unfreezable water content; w = water content; T_f = freezing point; T_m = temperature at which all free water freezes.

4 RESULTS

4.1 *Steady State vs. Transient Probe Method*

The thermal conductivity of the different soil samples was measured at room temperature using the transient probe

method, followed by the same soil sample being measured using the steady-state method to verify the thermal conductivity measurement using the modified heating cell. As shown in Figure 6, the thermal conductivity obtained from the steady-state method closely matches that measured by the standard transient probe (TR-1 probe) at room temperature, with the TR-1 probe showing a slight underestimation. The strong agreement of the measurement validates the accuracy of the thermal conductivity measurement based on the steady state method and demonstrates its potential as a reliable alternative to measure the thermal conductivity of the soils under more extreme freezing conditions, where the transient probe methods may be less reliable due to their heating requirement for thermal conductivity measurement.

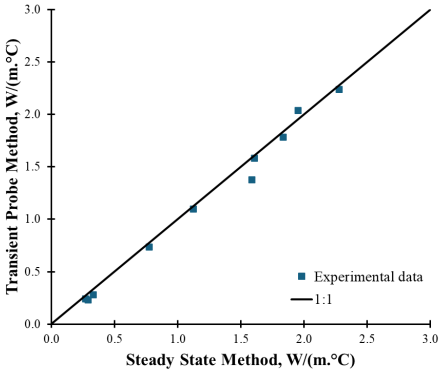

Figure 6. Thermal conductivity comparison from the transient probe method and the steady state method at room temperature.

4.2 *Thermal Conductivity of Benbrook Sand*

The recorded thermal conductivity of the moist Benbrook sand showed a positive correlation with temperature above the freezing temperature, as the thermal conductivity of the constituents of the soil, i.e., water, air, and solids, increased as well. Furthermore, there was a sharp rise in the thermal conductivity of the soil below the freezing point due to the rise of the thermal conductivity of unfrozen water (0.64 W/m.°C) to the frozen water (2.2 W/m.°C), followed by the gradual increase in thermal conductivity with temperature as more unfrozen pore water transitions into ice.

Among the three studied thermal conductivity models for the freezing soils, only the Cote and Konrad (2005) model could model the thermal conductivity from freezing to the elevated temperature, but showed poor correlation, as can be seen in Figure 7. Furthermore, Figures 8 and 9 show Wang et al. (2017) and Bi et al. (2023) best fit models on the experimental dataset, which show good correlation under freezing conditions, but the models were not capable of handling the elevated temperatures.

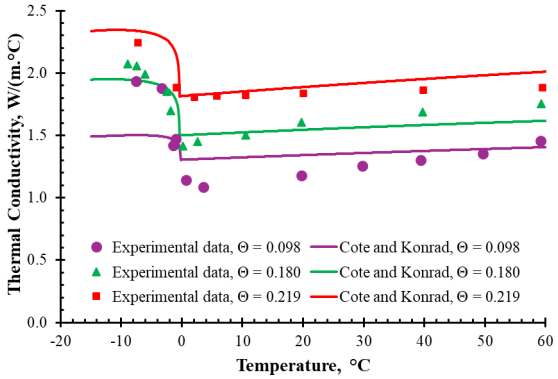

Figure 7. Thermal conductivity of Benbrook sand with fitted Cote and Konrad model.

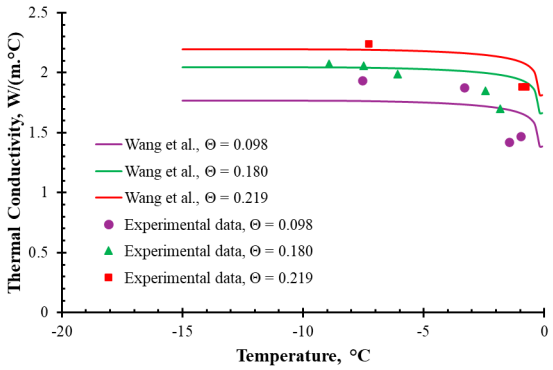

Figure 8. Thermal conductivity of Benbrook sand with the fitted Wang et al. model.

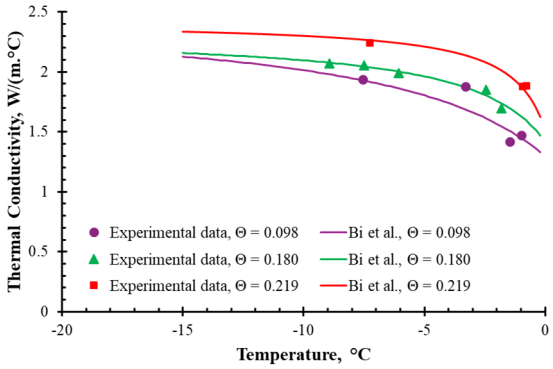

Figure 9. Thermal conductivity of Benbrook sand with the fitted Bi et al. model.

4.3 *Thermal Conductivity of ASTM C778 Sand*

The thermal conductivity of the Ottawa fine-graded sand was measured to be significantly higher than that of the Benbrook Sand at similar moisture content, density, and temperature due to the higher intrinsic thermal conductivity of the minerals. The thermal conductivity of the Ottawa sand also showed a positive temperature effect on the thermal conductivity above and below the freezing point of the soil, as can be seen from Figures 10 and 11. The thermal conductivity models from Cote and Konrad (2005) and Bi et al. (2023) demonstrated a good prediction for the freezing condition; however, Cote and Konrad (2005) failed to capture the true temperature effect at elevated temperatures.

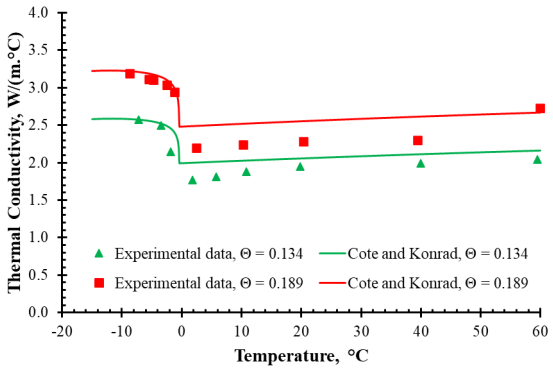

Figure 10. Thermal conductivity of Ottawa sand with fitted Cote and Konrad model.

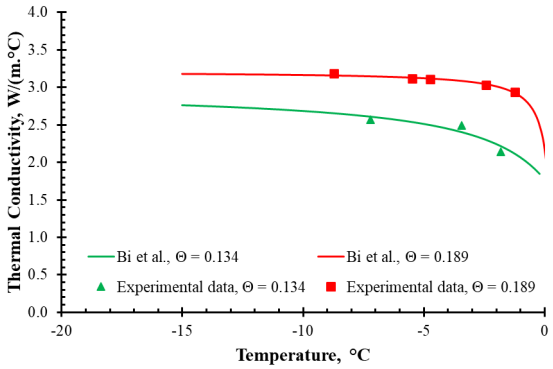

Figure 11. Thermal conductivity of Ottawa sand with the fitted Bi et al. model.

4.4 *Unfrozen Water Content*

Unfrozen water content dropped rapidly as the soil started to freeze, then showed a steady, smaller decline as the temperature continued to decrease, eventually reaching near the unfreezable water content. Among the two studied models, the Liu et al. (2013) model exhibited a sharp drop in the unfrozen water content with temperature below the freezing temperature and had poorer correlation with experimental data for high moisture content soil, as can be seen in Figure 12. However, the exponential-based model shown in Figure 13 by Kozlowski (2007) performed exceptionally well across all moisture contents and was selected for predicting unfrozen water content in thermal-conductivity models. Furthermore, Kozlowski's (2007) model performed well in predicting the unfrozen water content of the fine-graded Ottawa sand.

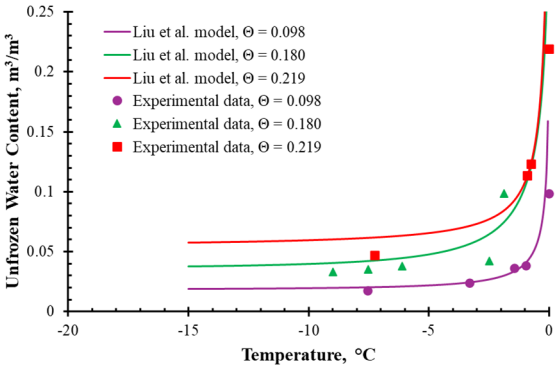

Figure 12. Unfrozen water content of Benbrook sand with the fitted Liu et al. model.

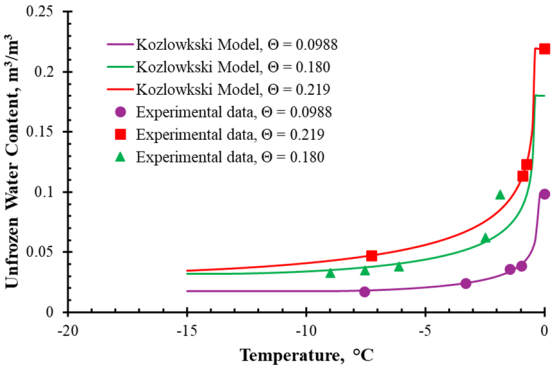

Figure 13. Unfrozen water content of Benbrook sand with fitted Kozlowski model.

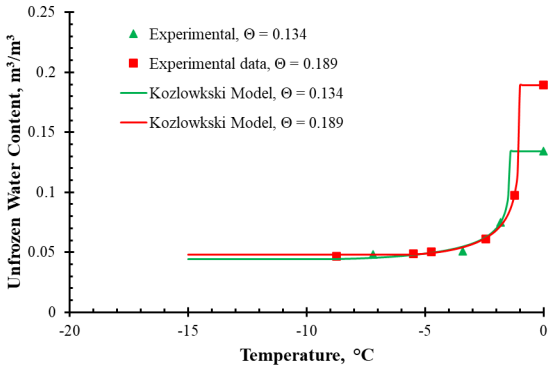

Figure 14. Unfrozen water content of freezing Ottawa sand with fitted Kozlowski model.

5 DISCUSSION

The unfrozen water content showed a rapid reduction below the freezing temperature, followed by a steady drop at a reduced rate when the temperature dropped further below -5°C. The unfrozen WC models also showed that the unfreezable water content in unsaturated soil increased with increasing soil moisture. Among the two SFCC models, the exponential model by Kozlowski (2007) performed better and captured the asymptotic nature of unfrozen water content in unsaturated soils without the rapid overprediction near 0°C, as observed in the Liu et al. (2013) SFCC model.

The thermal conductivity of the sandy soils showed a steady rise above 0°C in all soils, resulting from the increased intrinsic thermal conductivity of each phase and increased diffusion of the water vapor in pores. Furthermore, the reduction of the temperature below the freezing point showed a rapid increase in thermal conductivity due to the phase change of lower thermal conductivity water to higher thermal conductivity ice. The replacement of air-voids with an increased volume of the pore ice further resulted in increased thermal conductivity. The thermal conductivity increment of the frozen soil significantly dropped below 5°C due to the reduced phase change in the soil. The Cote and Konrad (2005) model was able to capture the thermal conductivity increment in freezing soil, but it underestimated the thermal conductivity of the soil in the thawed stage, likely due to the disregarded diffusive heat transfer in the soil.

For the soils under freezing conditions, Bi et al. (2023) showed exceptional correlation with the experimental data, whereas Wang et al. (2017) failed to capture the rapid increment of the thermal conductivity as seen from the experimental results. However, both models were incapable of predicting the thermal conductivity of thawed soils.

6 CONCLUSION

The thermal conductivity results of the soils based on the transient probe method by the TR-1 probe and the steady state method at room temperature validated the use of the steady state method for the thermal conductivity measurement, as the measurements from the two methods are close, with a slight underestimation of thermal conductivity from the transient probe method.

The unfrozen water content of the soil underwent a significant drop as the temperature decreased below the freezing point, which was perfectly modeled by Kozlowski's (2007) model based on optimized unfreezable water content and the temperature at which all free water freezes. Thus, the model could establish a continuous unfrozen water content with minimum errors.

However, the unified thermal conductivity model of soils by Cote and Konrad (2005) did not perform well under thawed conditions, and the true extent of the temperature effect on the thermal conductivity could not be captured. The thermal conductivity model for freezing soils, as presented by Bi et al. (2023), showed good correlation with thermal conductivity under freezing conditions; however, it lacked predictions at elevated temperatures.

7 ACKNOWLEDGEMENT

The authors would like to express their gratitude to the University of Texas at Arlington for providing the necessary resources to carry out this work.

8 REFERENCES

Alrtimi, A., Rouainia, M. & Manning, D.A.C., 2014, 'An improved steady-state apparatus for measuring thermal conductivity of soils', *International Journal of Heat and Mass Transfer*, 72, 630–636.

Alzoubi, M.A., Xu, M., Hassani, F.P., Poncet, S. & Sasmito, A.P., 2020, 'Artificial ground freezing: A review of thermal and hydraulic aspects', *Tunnelling and Underground Space Technology*, 104, 103534.

Anderson, D.M. & Tice, A.R., 1972, 'Predicting Unfrozen Water Contents in Frozen Soils from Surface Area Measurements'.

ASTM International, 2017, *Standard Practice for Classification of Soils for Engineering Purposes (Unified Soil Classification System)*.

Bi, J., Wu, Z., Cao, W., Zhang, Y., Wen, H., Yang, S., Zhang, Q., Sun, T. & Wei, T., 2023, 'A hyperbolic model for the thermal conductivity of freezing soils', *Geoderma*, 436, 116507.

Chen, Y., Min, Y., Jiang, H., Luo, J., Liu, M., Wang, E., Liu, X., Shi, K. & Li, X., 2025, 'Investigation on Thermal Conductivity of Soil Under Freeze–Thaw Action Based on Machine Learning Models', *Buildings*, 15(5), 750.

Côté, J. & Konrad, J.-M., 2005, 'A generalized thermal conductivity model for soils and construction materials', *Canadian Geotechnical Journal*, 42(2), 443–458.

Farouki, O.T., 1981, 'Thermal Properties of Soils'.

Fu, Y., Liu, L., Lu, Y., Horton, R., Ren, T. & Heitman, J., 2023, 'Estimating soil water retention curves from thermal conductivity measurements: A percolation-based effective-medium approximation', *Journal of Hydrology*, 624, 129898.

Genuchten, M.Th. van, 1980, 'A Closed-form Equation for Predicting the Hydraulic Conductivity of Unsaturated Soils', *Soil Science Society of America Journal*, 44(5), 892–898.

Hjort, J., Streletskiy, D., Doré, G., Wu, Q., Bjella, K. & Luoto, M., 2022, 'Impacts of permafrost degradation on infrastructure', *Nature Reviews Earth & Environment*, 3(1), 24–38.

Jin, X., Yang, W., Gao, X., Zhao, J.-Q., Li, Z. & Jiang, J., 2020, 'Modeling the Unfrozen Water Content of Frozen Soil Based on the Absorption Effects of Clay Surfaces', *Water Resources Research*, 56(12), e2020WR027482.

Johansen, O., 1977, 'Thermal Conductivity of Soils'.

Kozlowski, T., 2007, 'A semi-empirical model for phase composition of water in clay–water systems', *Cold Regions Science and Technology*, 49(3), 226–236.

Laloui, L. & Di Donna, A., 2013, *Energy geostructures: innovation in underground engineering*, John Wiley & Sons.

Liu, Z. & Yu, X. (Bill), 2013, 'Physically Based Equation for Phase Composition Curve of Frozen Soils', *Transportation Research Record*, 2349(1), 93–99.

Lunardini, V.J. & Laboratory (U.S.), C.R.R. and E., 1988, *Freezing of Soil with an Unfrozen Water Content and Variable Thermal Properties*, US Army Corps of Engineers, Cold Regions Research & Engineering Laboratory.

Orakoglu Firat, M.E., 2021, 'Experimental study and modelling of the thermal conductivity of frozen sandy soil at different water contents', *Measurement*, 181, 109586.

Putkonen, J., 2003, 'Determination of frozen soil thermal properties by heated needle probe', *Permafrost and Periglacial Processes*, 14(4), 343–347.

Sivaprasad, A. & Basu, P., 2023, 'Comparative assessment of transient- and steady-state soil thermal conductivity using a specially designed consolidometer', *Geothermics*, 107, 102583.

Spaans, E.J.A. & Baker, J.M., 1996, 'The Soil Freezing Characteristic: Its Measurement and Similarity to the Soil Moisture Characteristic', *Soil Science Society of America Journal*, 60(1), 13–19.

Tarnawski, V.R., Momose, T. & Leong, W.H., 2011, 'Thermal Conductivity of Standard Sands II. Saturated Conditions', *International Journal of Thermophysics*, 32(5), 984–1005.

Tarnawski, V.R. & Wagner, B., 1993, 'Modeling the thermal conductivity of frozen soils', *Cold Regions Science and Technology*, 22(1), 19–31.

Wang, L., Zhou, J., Qi, J., Sun, L., Yang, K., Tian, L., Lin, Y., Liu, W., Shrestha, M., Xue, Y., Koike, T., Ma, Y., Li, X., Chen, Y., Chen, D., Piao, S. & Lu, H., 2017, 'Development of a land surface model with coupled snow and frozen soil physics', *Water Resources Research*, 53(6), 5085–5103.

Weir, W.B., 1974, 'Automatic measurement of complex dielectric constant and permeability at microwave frequencies', *Proceedings of the IEEE*, 62(1), 33–36.

Zhao, T., Liu, S., Xu, J., He, H., Wang, D., Horton, R. & Liu, G., 2022, 'Comparative analysis of seven machine learning algorithms and five empirical models to estimate soil thermal conductivity', *Agricultural and Forest Meteorology*, 323, 109080.

Goering, D.J. (2003) "Passively Cooled Railway Embankments for Use in Permafrost Areas," *Journal of Cold Regions Engineering*, 17(3)